

# Infrared Temperature Sensing of Mechanically Loaded Specimens: Thermal Analysis

by Y. Rabin and D. Rittel

**ABSTRACT**—Infrared temperature-sensing techniques have the major advantages of virtually no interference of the sensor with the sensed phenomenon and fast inherent response. On the other hand, infrared temperature sensing, as a superficial measurement technique, does not indicate the specimen's core temperatures, and hence a complementary thermal analysis is required. A thermal analysis of surface temperature measurements of a mechanically loaded cylindrical specimen is presented. The specimen is modeled as an infinite cylinder, suddenly exposed to a uniformly distributed volumetric heat source. This heat source results from the conversion of mechanical energy into thermal energy. A closed-form solution is obtained and numerical examples are given for metallic and polymeric specimens. The current analysis provides the upper boundaries for temperature differences between the core and the surface temperatures when compared with the actual problem of a finite specimen. It is shown that surface temperature measurement is a good indication of the core temperature for metallic specimens but may lead to some poor results in the case of polymeric specimens. It is found that the transient thermal response of the infinite cylinder to sudden heating behaves like a first-order process. In the case of cyclic loading, the typical time scale of loading is found to be at least two orders of magnitude shorter than the typical time scale of heat transfer. Hence, the specimen is affected by the average power of heat generation, not the instantaneous effect of heating within a single loading cycle.

**KEY WORDS**—Infrared, temperature measurement, mechanical loading, time response, thermal analysis, mathematical model

## Introduction

Plastic deformations generate heat, which may raise the specimen's temperature. The effect of mechanical loading on the generated heat is widely reported in the literature in the context of monotonic<sup>1–9</sup> and cyclic<sup>10–13</sup> loading. Many efforts have been devoted to the evaluation of the thermal history during the mechanical loading, where the temperature was taken as an indicator of conversion of mechanical energy into thermal energy. The underlying assumption in these studies is that the difference between mechanically applied energy and the resulting thermal energy is the energy

stored into structural changes at either the micro level or the macro level. The accuracy in temperature measurement and the quality of the complementary thermal analysis are of great importance for understanding the coupled phenomena of mechanical stress, heat transfer and structural changes.

In general, temperature is a field property that is space and time dependant. Unfortunately, temperature measurement can be performed in either discrete points in space or, to some extent, on surfaces. Point sensors such as thermocouples, thermistors and Resistance Temperature Detectors (RTDs) can be applied for discrete temperature measurement, whereas liquid crystals and infrared measurement techniques are practical for superficial temperature measurement. The least accurate but most rapid response point sensor of the above list is the thermocouple,<sup>1,9</sup> which is also the most commonly applied. Rittel<sup>14</sup> presented a thermal analysis to gain some insight with regard to the transient response of solid-embedded thermocouples.

Infrared temperature measurement is commonly applied for superficial temperature measurement during mechanical loading.<sup>3,4,6,7,10</sup> With the appropriate calibration protocol, infrared temperature sensing is a very accurate temperature measurement technique, introducing virtually no interference between the sensor and the sensed phenomenon. In a heat transfer process associated with internal heat generation, one should expect to find the lowest temperatures at the outer surface. This may lead to an underestimation of the core temperature when measuring the superficial temperature, regardless of the accuracy of the particular measurement technique. Indeed, in testing,<sup>7</sup> it has been reported that temperatures somewhat lower than expected have been observed on the outer surface.

Consequently, the current study is intended to provide guidelines with regard to the thermal parameters under which the outer surface temperature closely represents the core temperature, compare the typical time scale of heat transfer with respect to the typical time scale of loading and provide numerical examples typical of metallic and polymeric specimens.

## Mathematical Formulation

For simplicity, the mathematical formulation is presented for a one-dimensional heat transfer process in the radial direction of an infinite solid cylinder. The infinite cylindrical model provides quite valuable results for the upper boundary of temperature differences between the core and the outer surface. The heat transfer problem is assumed to prevail by conduction in a cylinder of radius  $R$  driven by a uniformly distributed volumetric heat source  $\dot{q}$ :

---

*Y. Rabin is a Senior Lecturer, and D. Rittel (SEM Member) is a Senior Lecturer, Faculty of Mechanical Engineering, Technion-Israel Institute of Technology, Haifa 32000, Israel. Y. Rabin's current address, Associate Professor, Department of Mechanical Engineering, Carnegie Mellon University, Pittsburgh, PA.*

*Original manuscript submitted: June 22, 1999.*

*Final manuscript received: January 12, 2000.*

$$\nabla^2 T + \frac{\dot{q}}{k} = \frac{1}{\alpha} \frac{\partial T}{\partial t}, \quad (1)$$

where  $T$  is the temperature,  $t$  is the time,  $k$  is the thermal conductivity and  $\alpha$  is the thermal diffusivity. All thermophysical properties are assumed to be temperature independent and uniformly distributed in space.

The volumetric heat source is assumed to change as a steplike function:

$$\dot{q} = \begin{cases} 0 & t < 0 \\ \dot{q}_o & t \geq 0 \end{cases}. \quad (2)$$

In the case of cyclic loading, the actual heating power is expected to be cyclic in nature. However, it is shown below that a typical time scale of cyclic loading is a few orders of magnitude shorter than the typical time scale of heat transfer, and hence the thermal response follows the average power of heating and not the instantaneous variations within a single cycle.

Combined heat transfer by convection and radiation is assumed from the outer surface of the cylinder to the surroundings:

$$-k \frac{\partial T}{\partial r} \Big|_{r=R} = h (T|_{r=R} - T_\infty), \quad (3)$$

where  $T_\infty$  is the surroundings temperature and  $h$  is the combined heat transfer coefficient by convection and radiation.

For the purpose of this analysis, the Biot number is defined as

$$Bi = \frac{hR}{k}, \quad (4)$$

where  $Bi$  is a nondimensional parameter corresponding to the ratio of thermal resistance to heat transfer by conduction within the specimen's cross section and the thermal resistance to heat transfer by convection and radiation from the specimen's outer surface to the surroundings. The Fourier number is introduced as

$$Fo = \frac{\alpha t}{R^2}, \quad (5)$$

where  $Fo$  is a dimensionless time variable that is the normalizing parameter for transforming the heat conduction equation [eq (1)] into a dimensionless form.

The mathematical solution of the heat transfer problem defined in eqs (1)-(2) is the transient temperature distribution:

$$\theta \equiv T - T_\infty = \frac{\dot{q}_o R^2}{4k} \left[ 1 - \left( \frac{r}{R} \right)^2 + \frac{2}{Bi} - 8Bi \sum_{n=1}^{\infty} e^{-\gamma_n^2 Fo} \frac{J_0(\gamma_n r/R)}{\gamma_n^2 (Bi^2 + \gamma_n^2) J_0(\gamma_n)} \right], \quad (6)$$

where  $J_\nu$  is a Bessel function of order  $\nu$  and  $\gamma_n$  are the positive roots of the transcendental equation:

$$\gamma_n J_1(\gamma_n) - Bi J_0(\gamma_n) = 0, \quad (7)$$

and where eq (7) satisfies the boundary condition presented by eq (3).<sup>15</sup>

For purposes of this analysis, let us redefine the transient temperature difference  $\theta$  [eq (6)] in the dimensionless form  $\phi$  as the sum of a steady-state temperature distribution  $\phi_{ss}$  and a time-dependent term  $\phi_{td}$  as follows:

$$\begin{aligned} \phi &\equiv \frac{4k\theta}{\dot{q}_o R^2} \\ \phi &= \phi_{ss} + \phi_{td} \\ \left\{ \begin{aligned} \phi_{ss} &= 1 - \left( \frac{r}{R} \right)^2 + \frac{2}{Bi} \\ \phi_{td} &= -8Bi \sum_{n=1}^{\infty} e^{-\gamma_n^2 Fo} \frac{J_0(\gamma_n r/R)}{\gamma_n^2 (Bi^2 + \gamma_n^2) J_0(\gamma_n)} \end{aligned} \right. \end{aligned} \quad (8)$$

Note that the dimensionless temperature  $\phi$  is independent of the heating power  $\dot{q}_o$ , the thermal conductivity  $k$  and the radius  $R$ . The transient temperature distribution is dependent on  $Bi$ ,  $Fo$  and the radii ratio only.

For practical reasons, the infinite series shown in eq (8) is truncated after the sixth term in the current numerical analysis, which results in a dimensionless temperature error of less than  $10^{-4}$ .

## Thermal Analysis

Following the presentation of the temperature distribution in eq (8), it seems convenient to discuss the steady-state temperature distribution separately from the transient temperature response. It is shown below that the analysis of the steady-state temperature distribution leads to some general and important conclusions.

### Steady-state Temperature Distribution

The steady-state temperature distribution, where  $\phi = \phi_{ss}$  and  $\phi_{td} = 0$ , is a function of  $Bi$  and the radii ratio only. It can be seen from eq (8) that the maximal value of the dimensionless temperature  $\phi_{ss}$  is found at the center of the cylinder. The value of the maximal temperature is inversely proportional to the value of the  $Bi$  number. On the other hand, the value of the dimensionless temperature difference between the center of the cylinder and its outer surface equals 1, regardless of the  $Bi$  value. For example,  $\phi_{ss}$  varies between 201 at the center of the cylinder and 200 at its outer surface for a  $Bi$  value of 0.01. Similarly,  $\phi_{ss}$  varies between 1.2 at the center of the cylinder and 0.2 at its outer surface for a  $Bi$  value of 10. This means that at steady state, when estimating the core temperature of the cylinder with surface temperature measurements, an error of up to 0.5 percent is introduced for a  $Bi$  value of 0.01 whereas an error of up to 80 percent is introduced for a  $Bi$  value of 10.

Figure 1 shows the ratio of the temperature at the outer surface of the cylinder to the temperature at its center in steady state, where this ratio is defined by

$$\eta(Bi) \equiv \frac{\theta(r=R, t \rightarrow \infty)}{\theta(r=0, t \rightarrow \infty)} = \frac{\phi_{ss}(R)}{\phi_{ss}(0)}. \quad (9)$$

It can be concluded from Fig. 1 that for  $Bi$  values of 0.01, 0.1, 1, 10 and 100, the underestimation of the center temperature, when sensing the outer surface temperature, is

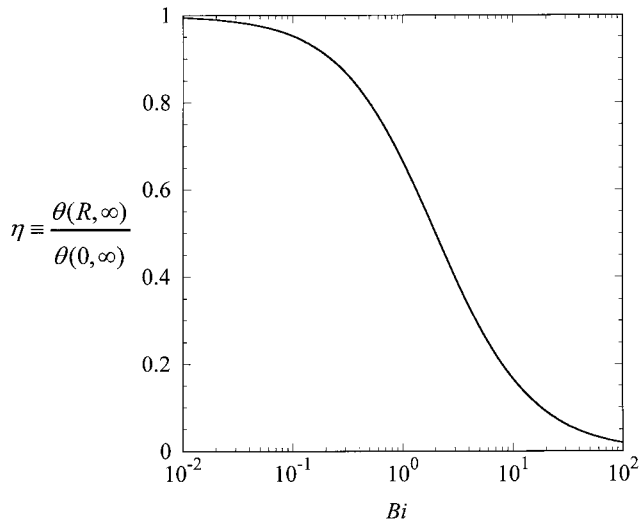


Fig. 1—Steady-state ratio of the outer surface temperature to the core temperature,  $\eta$  [eq (10)]. Higher values of  $\eta$  represent higher radial temperature uniformity

0.5 percent, 5 percent, 37 percent, 83 percent and 98 percent, respectively. This coincides with the engineering rule of thumb that the temperature distribution can be approximated as uniform for  $Bi \leq 0.1$ .

### Transient Temperature Distribution

The dimensionless transient temperature distribution, where  $\phi = \phi_{ss} + \phi_{td}$  and  $\phi_{td} \neq 0$ , is a function of the following dimensionless parameters:  $Bi$ , the radii ratio and  $Fo$ . In Fig. 2, the transient temperature distribution  $\phi$  is shown as a function of the radii ratio for constant  $Fo$  intervals and for three representative values of  $Bi$ . The upper temperature distribution in each figure corresponds to the steady-state temperature distribution discussed above, that is,  $Fo = \infty$ . It can be seen from Fig. 2(a) that for a  $Bi$  value of 0.1, a relatively uniform temperature distribution is found at a steady state and an almost uniform temperature distribution is observed during the transient process. On the other hand, for higher  $Bi$  values [Figs. 2(b) and 2(c)], the radial temperature gradients become significantly steeper with time and the temperature difference between the center and the outer surface is found to be maximal at a steady state. It can be concluded that the poorest underestimation of the core temperature by surface temperature measurements occurs when the transient process approaches steady state.

### Time Response to Heat Generation

It can be seen from eq (6) that the temperature distribution is exponentially dependent in time; hence, one should expect the temperature to behave similarly to a first-order process. For the purpose of this analysis, let us define the ratio of the transient temperature distribution to the steady-state temperature distribution for a given radius as

$$\zeta(r/R, Fo, Bi) \equiv \frac{\theta(r/R, Fo, Bi)}{\theta_{ss}(r/R, Bi)} = \frac{\phi_{td} + \phi_{ss}}{\phi_{ss}}, \quad (10)$$

where it is known that for an ideal first-order process,

$$(Fo @ \zeta = 1 - e^{-1}) = \frac{1}{n} (Fo @ \zeta = 1 - e^{-n}). \quad (11)$$

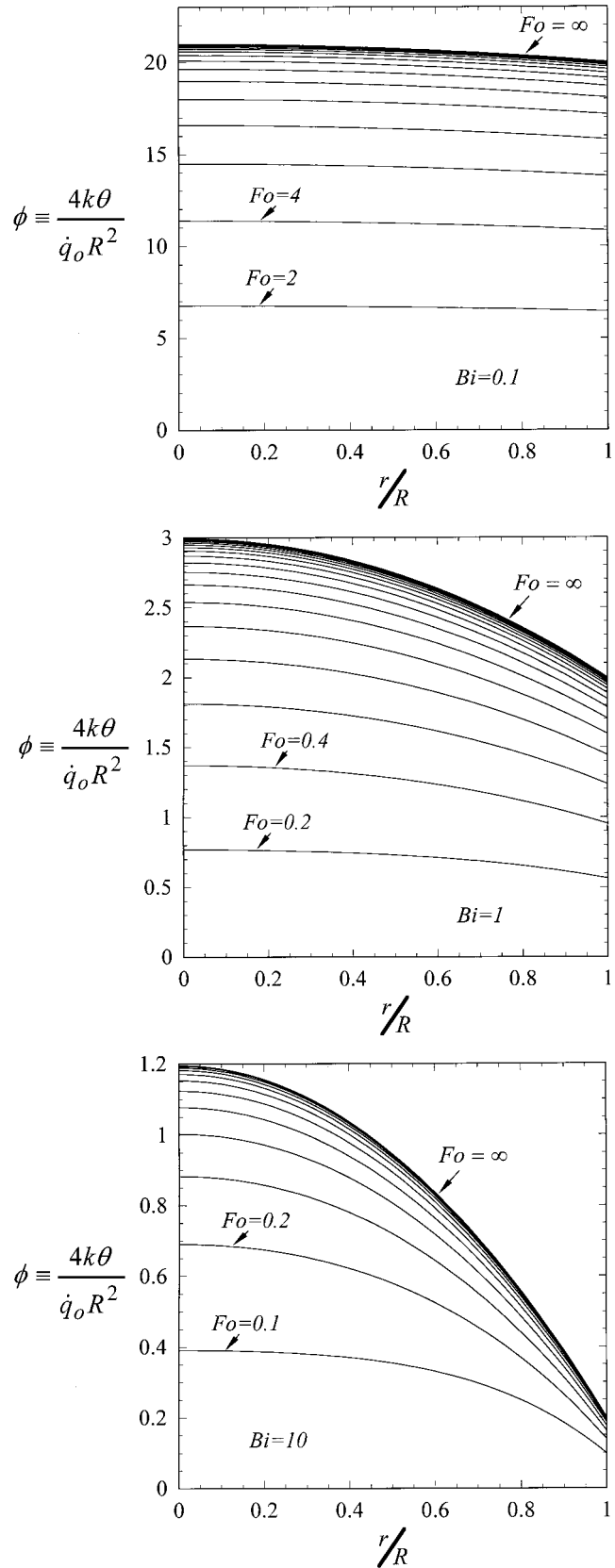


Fig. 2—Radial temperature distribution [eq (6)] for the case of (a)  $Bi = 0.1$ , (b)  $Bi = 1$  and (c)  $Bi = 10$  drawn in 2, 0.2 and 0.1  $Fo$  increments, respectively ( $Fo = \infty$  at steady state).  $Bi$  values of 0.1 to 10 are typical for polymers, whereas  $Bi$  values of less than 0.1 are typical for metals

TABLE 1—DIMENSIONLESS TIME VARIABLE  $Fo$  AT WHICH THE DIMENSIONLESS TEMPERATURE RATIO  $\zeta$ , DEFINED IN EQ (10), REACHES SOME SPECIFIC VALUES AT THE CENTER OF THE CYLINDER

	$Bi = 0.01$	$Bi = 0.1$	$Bi = 1$	$Bi = 10$	$Bi = \infty$
$\zeta(0) = 1 - e^{-1} = 0.632$	50.2	5.13	0.64	0.230	0.197
$\zeta(0) = 1 - e^{-2} = 0.865$	100.4	10.26	1.28	0.441	0.376
$\zeta(0) = 1 - e^{-3} = 0.950$	150.6	15.39	1.92	0.652	0.555

Table 1 lists the dimensionless time  $Fo$  at which the ratio  $\zeta$  at the center of the cylinder reaches some specific value. It can be seen from Table 1 that for small  $Bi$  values (e.g., up to 1), the transient response at the center of the cylinder behaves similarly to a first-order response, in accordance with eq (11).

As mentioned earlier, the radial temperature variation is insignificant for a  $Bi$  value of up to 0.1. Thermal systems characterized by such a low  $Bi$  value are known as lumped-heat capacity systems, where a uniform temperature distribution may be assumed. The time constant of a lumped-heat capacity system is defined as<sup>15</sup>

$$\frac{t}{\tau} \equiv \frac{hAt}{CV} = \frac{2ht}{CR} = 2BiFo, \quad (12)$$

where  $\tau$  is the dimensional time constant,  $V$  is the volume of the system,  $A$  is the surface area exposed to the surroundings and  $C$  is the volumetric-specific heat. It follows that the production of  $2BiFo$  equals  $n$  after  $n$  time constants. Indeed, it can be seen from Table 1 that when  $\zeta$  reaches the value of  $1 - e^{-1}$ , that is, after one time constant, the value of  $2BiFo$  reaches 1.004 and 1.026 for  $Bi$  values of 0.01 and 0.1, respectively. For a  $Bi$  value of 1, however, a value of 1.28 is found for  $2BiFo$ , which is significantly different than the same value in the idealized first-order system. For the case of a low  $Bi$  value, eq (12) can be further simplified to

$$\tau = \frac{CR}{2h}. \quad (13)$$

It is concluded that the transient temperature at the center of the cylinder behaves like a first-order process for a  $Bi$  value of up to 1. It is further concluded that the time constant of this process can be approximated from eq (13) for a  $Bi$  value of up to 0.1.

### Boundary Conditions

The underlying assumption of this analysis is that the thermal problem can be modeled as one-dimensional in the radial direction of an infinite solid cylinder. However, the actual cylindrical specimen has finite dimensions, where the diameter and length may sometimes be of the same order of magnitude. One may argue that the end effect in such a heat transfer problem cannot be ignored, and therefore the validity of this analysis is questioned. Hence, the relation between the infinite model and the finite specimen is addressed.

The bases of the cylindrical specimen are loaded by metallic platens in compression testing or by grips in tension testing. In some cases of compression testing, thermal insulation plates, such as ceramic plates,<sup>12,13</sup> are placed between the specimen and the metallic platens to reduce heat transfer by conduction to the platens. When analyzing the case of no thermal insulation, the following factors should be taken into account. The platens and grips are made of metallic materials, and their thermal conductivity is no less than that of the specimen. It follows that the thermal resistance to heat transfer by

conduction in the platens or grips along the specimen's bases is expected to be no higher than that of the specimen. This should force the temperature gradients in the radial direction and on the specimen's bases to be more moderate than they are at the mid-height of the specimen. Furthermore, because the platens or grips are conducting heat to the high thermal mass of the loading device, the temperatures of the specimen bases are expected to be lower and more uniform when compared with the mid-height temperatures of the specimen. It can be concluded that the temperature difference between the center and the outer surface of an idealized model of an infinite cylinder represents an upper boundary for the same radial temperature difference in the finite specimen.

If the thermal insulation plates had provided perfect insulation, then by definition the finite specimen would have behaved like an infinite cylinder from heat transfer considerations in the case of thermal insulation. In reality, the thermal insulation is not perfect and the thermal results of the thermally insulated specimen should lie in between the results of the noninsulated case and the results of the idealized model of an infinite cylinder.

### Infinite Bars with Other Cross Sections

The mathematical formulation and the thermal analysis up to this point have focused on an infinite solid cylinder and on the relation between the infinite- and finite-length cases. One might wonder whether the thermal analysis presented in this report is applicable for infinite bars having other cross-sectional shapes. Of course one could rewrite the mathematical formulation for any given cross-sectional shape and attempt to derive a closed-form solution for that problem. On the other hand, because the results presented here are rather general, and because the analysis is dealing with an order-of-magnitude analysis, it is of great importance to be able to apply the results of the current thermal analysis to other cross-sectional shapes. One must remember that the mathematical formulation is presented in a dimensionless form as a function of  $Bi$ ,  $Fo$  and the dimensionless radii ratio. When considering an infinite solid bar of a different cross-sectional shape, one-half of the characteristic thickness of the bar can be taken instead of the radius  $R$  as the characteristic length for the calculation of  $Bi$  and  $Fo$ . Then, based on the values of these numbers, the thermal analysis presented above can serve as an engineering approximation for the new cross-sectional shape. The same characteristic length can be applied for the evaluation of the time constant  $\tau$  as well.

For the application of the current analysis to a hollow bar case, the characteristic length is the typical thickness of the walls, which is the difference between the outer and inner radii in the case of a hollow cylinder.

### Numerical Examples

Assuming a combined heat transfer coefficient by convection and radiation,  $h$ , in the range of 15 to 50  $W/m^2-^{\circ}C$  and a cylinder radius in the range of  $10^{-3}$  to  $10^{-2}$  m,  $Bi$  for

polymers is typically in the range of 0.1 to 10 ( $k_{\text{polymer}} = 0.1 \div 0.3 \text{ W/m} \cdot ^\circ\text{C}$ ). Under the same conditions,  $Bi$  is typically on the order of  $10^{-3}$  for industrial metals and  $10^{-5}$  for pure metals ( $k_{\text{carbon steel 1 percent}} = 43$ ,  $k_{\text{copper}} = 384 \text{ W/m} \cdot ^\circ\text{C}$ ).

### Metallic Specimens—Low $Bi$ Numbers

A  $Bi$  value of less than  $10^{-3}$  is typical for metallic specimens. As discussed above, the maximal temperature difference in the radial direction is between the center of the cylinder and its outer surface. Furthermore, this temperature difference at steady state is the upper boundary for the same temperature difference in the transient process. From eq (8), one can see that  $\phi_{ss}$  varies in the range of 2000 at the outer surface of the cylinder and 2001 at the center of the cylinder for a  $Bi$  value of  $10^{-3}$ . This means that a temperature difference of up to 0.05 percent is expected in industrial metals due to a sudden loading. Due to a lower typical value of  $Bi$ , the same temperature difference is far less significant for pure metals.

It is shown above that the thermal response of an infinite cylinder behaves like a first-order process for such low  $Bi$  values as those of metals. The typical specific heat of metals is in the range of  $2.5$  to  $3.5 \text{ MJ/m}^3 \cdot ^\circ\text{C}$ . It can be calculated from eq (13) that the typical time constant for metals is in the range of 102 to 103 s. One may conclude that the maximal temperature difference between the core and the outer surface presented above for short periods of loading (e.g., for a few fractions of a second at high strain rate experiments of monotonic loading) is greatly overestimated. It can be concluded further that in the case of a cyclic load test, the thermal response of the specimen is related to the average heating power and not to the instantaneous heating during a single cycle. This conclusion has implications with regard to heat transfer numerical simulations of mechanical loading; that is, there is no need to trace the cyclic heating power during the experimentation, and the average heating power over the typical time constant can be taken as constant without significantly affecting the accuracy of calculations.

### Polymeric Specimens—High $Bi$ Numbers

The typical value of  $Bi$  for polymeric specimens is in the range of 0.1 to 10. It can be calculated from eq (8) that an underestimation of 5 percent, 50 percent and 83 percent is expected at steady state for  $Bi$  values of 0.1, 1 and 10, respectively. Hence, an infrared temperature measurement of a polymeric specimen may lead to some poor results with regard to the core temperature.

A significant temperature variation can be observed for typical  $Bi$  values of polymeric specimens (see Fig. 2). For a  $Bi$  value of 1, for example [Fig. 2(b)], the underestimation of the core temperature by the surface temperature measurements is 37 percent, 44 percent, 48 percent and 50 percent at  $Fo$  values of 0.2, 0.4, 0.8 and  $\infty$ , respectively. This underestimation decreases with the decrease in  $Fo$  value and may be tolerable at the very short term, as is the case in impact tests. For purposes of experimental design, Fig. 3 shows the dependency of  $Fo$  in  $Bi$  for a dimensionless temperature difference of 3 percent, 5 percent and 10 percent between the core and the outer surface:

$$\varphi \equiv \frac{\theta(r = R) - \theta(r = 0)}{\theta(r = R)}, \quad (14)$$

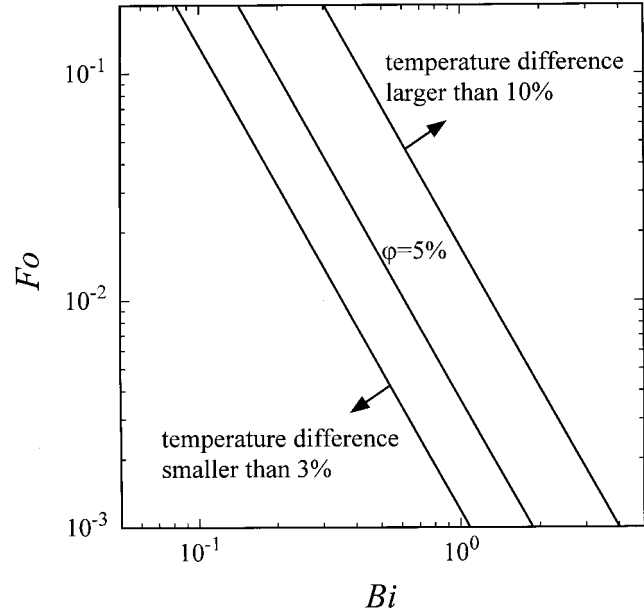


Fig. 3—The dependency of  $Fo$  in  $Bi$  for a dimensionless temperature difference of 3 percent, 5 percent and 10 percent between the core and the outer surface [eq (14)]

where  $\varepsilon$  is the dimensionless temperature difference between the core and the outer surface. For  $Bi$  values of less than 0.06, 0.1 and 0.2, the dimensionless temperature difference between the core and the outer surface is always less than 3 percent, 5 percent and 10 percent, respectively, regardless of the value of  $Fo$ . Using Fig. 3, one can estimate the time period in which a specific level of confidence is required when estimating the core temperature by surface temperature measurements. For example, for the case of a  $Bi$  value of 1, a temperature difference of 3 percent, 5 percent and 10 percent is found when  $Fo$  reaches the values of  $1.7 \times 10^{-3}$ ,  $4.5 \times 10^{-3}$  and  $2 \times 10^{-2}$ , respectively. For the specific case of a polymeric specimen having a radius of 5 mm, these  $Fo$  values correspond to time points of 0.43 s, 1.13 s and 5 s, respectively.

To capture the radial temperature distribution for polymeric specimens, temperatures should be measured at a few radial locations regardless of the specific temperature sensors employed. While the outer surface can be measured with an infrared measurement technique, the inner temperatures have to be measured with point sensors such as thermocouples, thermistors and RTDs. In the absence of such complementary measurements of inner temperatures, the thermal analysis of mechanical loading of polymeric specimens characterized by high values of  $Bi$  is baseless unless the load is applied rapidly as discussed above.

One may conclude that  $Bi$  is an important experimental design parameter for which a value of no greater than 0.1 is preferred. It is suggested that the  $Bi$  value be routinely reported with other experimental data as an indicator of the temperature distribution uniformity.

The specific heat of polymers is typically in the range of  $0.5$  to  $1.5 \text{ MJ/m}^3 \cdot ^\circ\text{C}$ , which may lead to a typical time constant of heating in the range of 10 to 103 s. Again, as in the case of metals, the typical time scale of loading is longer than the typical time scale of the thermal response, and the average effect of heating can be taken over a few loading cycles for

numerical analysis of data obtained in cyclic testing. However, at extremely low loading frequencies (e.g., less than 1 Hz), the typical time scale of loading may be of the same order of magnitude as that of the thermal time scale. Therefore, the use of the thermal time constant as a design parameter of a specific experimentation is recommended. Furthermore, the time scale of the heat transfer process should be reported routinely with the other reported data.

## Summary and Conclusions

Thermal analysis of a mechanically loaded cylindrical specimen is presented. The analysis assumes heat transfer by conduction in the specimen, uniformly distributed volumetric heat generation due to mechanical loading, uniform initial temperature distribution and combined heat transfer by convection and radiation to the surroundings. The specimen is modeled as an infinite cylinder for which a closed-form solution is obtained and presented in a dimensionless form. The dimensionless temperature distribution is independent of the power of heating. Results of this analysis are rather general and can be applied to infinite bars of other cross-sectional shapes.

Surface temperature measurements such as infrared measurements always underestimate the core temperature. For metals, however, the dimensionless temperature difference between the core and the outer surface is up to 0.05 percent. It is concluded that surface temperature measurement is a good indicator of the core temperature of a metallic specimen. For polymers, on the other hand, the dimensionless temperature difference between the outer surface and the core may be as high as 80 percent. It is concluded that the temperature distribution has to be measured in several radial locations for the case of a polymeric specimen in order to capture the radial temperature distribution. Hence, surface temperature measurement alone may lead to a poor estimation of the radial temperature distribution in a polymeric specimen.

It is shown that the infinite cylindrical model applied in this analysis provides the upper boundary for radial temperature differences when compared with the actual problem of a finite specimen. This means that the underestimation of the core temperature when measuring the surface temperature is not higher than one that is calculated based on the infinite cylindrical model.

The transient temperature response to a steplike heat generation process behaves like a first-order response. In the case of cyclic loading of a metallic specimen, the typical time scale of loading is found to be at least two orders of magnitude shorter than the typical time scale of heat transfer. Hence, the specimen is affected by the average heating power and not by the instantaneous heating power within a single

loading cycle. In the case of cyclic loading of a polymeric specimen, the typical time scale of loading may exceed the typical time scale of heat transfer in some extreme conditions. The typical value of the thermal time constant can be used as a guide to find a time period for averaging the thermal effect of cyclic loading when simulating the coupled phenomena of mechanical loading and heat generation. This can save numerical simulation efforts and computer running time.

## Acknowledgments

The first author acknowledges the support of the Stanley Imerman Memorial Academic Lectureship. The second author acknowledges the support of the Israel Science Foundation (Grant No. 030-039). The authors would like to thank Miriam Webber for assistance in the preparation of this paper.

## References

1. Chou, S.C., Robertson, K.D., and Rainey, J.H., "The Effect of Strain Rate and Heat Development During Deformation on the Stress-strain Curve of Plastics," *EXPERIMENTAL MECHANICS*, **13**, 422–432 (1973).
2. Lee, H.T. and Chen, J.C., "Temperature Effect Induced by Uniaxial Tensile Loading," *J. Mat. Sci.*, **26**, 5685–5692 (1991).
3. Haward, R.N., "Heating Effects in the Deformation of Thermoplastics," *Thermochimica Acta*, **247**, 87–109 (1994).
4. Mason, J.J., Rosakis, A.J., and Ravichandran, G., "On the Strain and Strain Rate Dependence of the Fraction of Plastic Work Converted to Heat: An Experimental Study Using High Speed Infrared Detectors and the Kolsky Bar," *Mech. Mat.*, **17**, 135–145 (1994).
5. Salamatina, O.B., Höhne, G.W.H., Rudven, S.N., and Oleinik, E.F., "Work, Heat and Stored Energy in Compressive Plastic Deformation of Glassy Polymers," *Thermochimica Acta*, **247**, 1–18 (1994).
6. Arruda, E.M., Boyce, M.C., and Jayachandran, R., "Effects of Strain Rate, Temperature, and Thermomechanical Coupling on the Finite Strain Deformation of Glassy Polymers," *Mech. Mat.*, **19**, 192–212 (1995).
7. Kapoor, R. and Nemat-Nasser, S., "Determination of Temperature Rise During High Strain Rate Deformation," *Mech. Mat.*, **27**, 1–12 (1998).
8. Noble, J.P., Goldthorpe, B.D., Church, P., and Harding, J., "The Use of the Hopkinson Bar to Validate Constitutive Relations at High Rates of Strain," *J. Mech. Phys. Solids*, **47**, 1187–1206 (1999).
9. Riddell, M.N., Koo, G.P., and O'Toole, J.L., "Fatigue Mechanisms of Thermoplastics," *Polymer Eng. Sci.*, 363–368 (Oct. 1966).
10. Birman, V., "On the Effect of Cyclic Loading on Material Temperature," *Mech. Res. Communications*, **25**, 653–660 (1998).
11. Rittel, D., "An Investigation of the Heat Generation During Cyclic Loading of Two Glassy Polymers, Part I: Experimental Study," *Mech. Mat.*, **32**, 131–147 (2000).
12. Rittel, D. and Rabin, Y., "An Investigation of the Heat Generation During Cyclic Loading of Two Glassy Polymers, Part II: Thermal Analysis," *Mech. Mat.*, **32**, 149–159 (2000).
13. Rabin, Y. and Rittel, D., "A Model for the Time Response of Solid-embedded Thermocouples," *EXPERIMENTAL MECHANICS*, **39**, 132–137 (1999).
14. Rittel, D., "On the Conversion of Plastic Work to Heat During High Strain Rate Deformation of Glassy Polymers," *Mech. Mat.*, **31**, 131–139 (1999).
15. Carslaw, H.S. and Jaeger, J.C., *Conduction of Heat in Solids*, 2nd ed., Oxford University Press, Oxford, 205 (1959).